Plane Wave Diffraction Problem Analysis using Microwave Technology and with Application for Breast Scanning

Emine Avşar Aydin
1- Adana Alparslan Türkeş Science and Technology University, Department of Aerospace Engineering, Adana, Turkey.
Email: eaydin@atu.edu.tr or rasvaenime@gmail.com

Received: August 2020 Revised: October 2020 Accepted: November 2020

ABSTRACT:
This paper presents an analytical solution to the problem of non-invasively detecting an object in a medium using a microwave signal applied from the surface. This solution is based on the one and two-dimensional microwave inverse calculation methods. Since the dielectric properties of the object and the medium are different from each other, the backscattered electromagnetic waves can characterize the properties of the object and the medium. The impedance and reflection coefficients are calculated from the forward and backscattered signals as a function of the frequency. An analytical-numerical method is developed to analyze how an H-polarized plane wave is diffracting from two axisymmetric infinitely long strips located at the z-axis and have the same width. A straightforward solution to a problem difficult to solve is presented using hybrid analytical-numeric methods. Detecting tumors in breast tissue is one of the critical areas that the method will be effectively used. The solution is successfully applied to the breast tissue to detect the tumor inside it. Different scenarios are presented along with their numerical examples and radar cross-section data. From the insight obtained from these numerical examples, the scattering characteristics of the far-field are discussed to emphasize the contribution of the presented solution.

KEYWORDS: Analytic, Breast Layers, Diffraction, Numeric, Strip.

1. INTRODUCTION

Given the deaths it causes, breast cancer, which has become a serious problem for all women, occurs in breast tissue, and spreads through the chest muscles [1]. Each breast consists of milk channels, mammary glands, and adipose tissue and contains 15 to 20 independent milk-producing tissues called lobes. Each lobe has 20 to 40 smaller sub-tissues called lobules; each lobule is also divided into several sections, the so-called alveoli, in which the primary milk-producing cells are collected. The milk produced is transported from the alveoli to milk ducts and from there to larger ducts. The gaps between the lobules and the milk ducts are filled with adipose tissue, as shown in Figure 1 [2]. The structure of each woman's breast is different due to their menstrual cycle, and tissue varies according to age. For example, young women have mammary glands and milk ducts in their breast tissue, while older women have mostly adipose tissue.

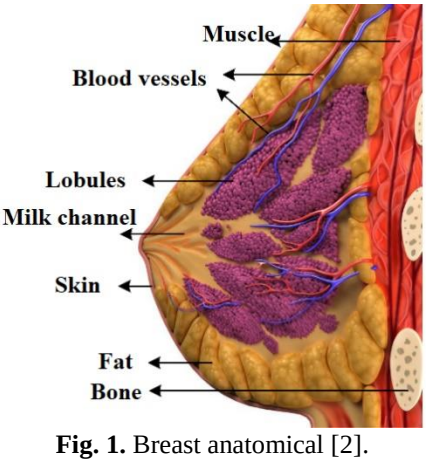

Fig. 1. Breast anatomical [2].

The main reason for the development of breast cancer is mutating at the genes that control the growth of cells [1]. A healthy cell know when and where to divide. In contrast, these unconscious cells divide in an uncontrolled manner to form cancerous cells. Breast cancer usually occurs in lobules or milk ducts.

According to 2009 data, the distribution of causes of death in Turkey by gender is given in Table 1 [3]. As

Paper type: Research paper
DOI: https://doi.org/10.29252/mjtd.9.4.167
How to cite this paper: E. Avşar Aydin, **"Plane Wave Diffraction Problem Analysis Using Microwave Technology and with Application for Breast Scanning"**, *Majlesi Journal of Telecommunication Devices*, Vol. 9, No. 4, pp. 167-176, 2020.

seen from the table, cancer ranks second after cardiovascular problems (heart and blood vessel related) in Turkey. While the average cancer-related mortality rate was 12% in 2002 [4], it increased to 20.2% in 2009. Again, according to the same research [3, 4], cancer-related deaths, which are ranked 2nd in the world (according to 2009 data), are expected to rise to the first place since 2015.

Table 1. Distribution rate compared to 2009 data by gender of deaths in Turkey [3].

Cause of death	Percentage (%)	
	Male	Female
Cardiovascular diseases	36.2	44.4
Cancer	24.4	16
Respiratory diseases	10.1	7.4
Metabolic diseases	4.8	8.3
Poisoning and trauma	4.9	2.8
Other	19.6	21

Cancers can develop in various tissues and are named according to the tissue in which they develop. The incidence of cancer types by gender is shown in Table 2.

Table 2. Frequency of cancer according to gender [3].

Male		Female	
Cancer Type	%	Cancer Type	%
Lung	69.2	Breast	40.7
Prostate	37.6	Thyroid	16.2
Bladder	21.7	Colorectal	13.2
Colorectal	20.8	Uterine Corpus	8.6
Stomach	18	Lung	8.2
Larinks	9.1	Stomach	7.7
NHL	6.9	Over	6.9
Brain, nervous system	6.1	NHL	5
Pancreas	6.1	Brain, nervous system	4.4
Kidney	5.8	Cervix	4.1
Thyroid	3.9	Bladder	3
Breast	0.8	Larinks	0.5

Early diagnosis significantly reduces deaths due to breast cancer, which is the most common after lung cancer in the world. Various methods have been developed to detect and visualize cancerous tissues. Detection of breast cancer using electromagnetic waves can be achieved by electromagnetic contrast between the breast tissue and tumor and/or by electrical signals generated by cancerous cells [5]. Because of this feature of breast tissue, the microwave has found itself in the detection and imaging of breast cancer.

Breast screening methods should consider patients' comfort, high-resolution images, cost, and accuracy of malignant masses [6]. Various techniques are available for breast cancer detection. X-ray mammography is the most used method among these methods and based on x-ray imaging.

X-rays are electromagnetic waves in the energy range of 0.125 ~ 125 keV, wavelengths in the range of 10 to 0.01 nm (30 to 30,000 PHz (Petahertz)), and maybe detrimental because they belong to the ionizing radiation class [7]. The use of ionizing radiation in x-ray mammography is a disadvantage of this method. Another disadvantage of the method is that the necessity of compressing the breast for better imaging. This compression procedure makes the method uncomfortable to use both for the technician and the patient [5]. Some limitations in X-ray mammography, such as being uncomfortable due to the compression and the use of low power x-ray to minimize the damage, are the major problems in the correct detection of the tumor. These constraints have motivated the development of alternative techniques. However, the fact that these alternative techniques have various problems in themselves ensures the continuity of the studies on this subject [5]. An alternative method to X-ray mammography is magnetic resonance imaging (MRI). MRI offers high sensitivity but has a high cost and low specificity that can lead to reverse diagnosis. Therefore, in breast cancer detection, MRI is only preferred for high-risk situations. In addition, the long duration of the MRI imaging procedure also might disturb the patient [5].

Microwave imaging is one of the most recent breast cancer detection and imaging techniques [6, 8 - 10] and has great potential as a safe and efficient screening method. Studies in the literature have shown that microwave imaging is safer and cheaper than other methods used for breast cancer detection [11].

In this study, a hybrid method is proposed that can be used to identify tumor tissue inside the breast. The behaviors of a uniform plane wave that penetrates thought the breast are analyzed to find how deep the tumor from the surface of the breast.

In terms of the diffraction theory, the solutions of the scattering of canonical forms such as half-plane, cylinder, sphere, etc. are important. A strip is also a canonical form that is frequently used in the analysis of scattering. Besides, it can be used in the simulations of many practical problems involving remote sensing. The scattering around a slit can be modeled with the strip approach. Due to its suitability to numerous practical problems, the scattering of strip is widely researched by using various analytical and numerical methods [13-21].

As known, the electrical extent of the scattered limits the applicability of the numerical methods and the complexity of its form restricts the applicability of the analytical methods. Thus, hybrid methods are mostly being used for the asymptotic solution of the problem in

high frequencies. Hybrid methods include the utilization of the Geometrical Theory of Diffraction (GTD) and the Moment Method (MM) [22-24] as well as the Physical Theory of Diffraction (PTD) and the Moment Method (MM) [25].

Veliev proposed an alternative method to the literature [26]. Within his analytical-numerical method, the equation achieved in the spectral space is reduced to a system of linear equations in terms of the unknown Fourier coefficients of the current density function which is induced on the scatterer. By using the calculated coefficients, the surface current density function and, consequently, the field expression and the radar cross-section can be determined. The problem of an impedance strip was solved by using this method [12]. The basis of the method is the reduction of the integral equation in spectral space to the system of linear equations and contains the analytical solution of the integrals. There is mathematical complexity in this stage of the method.

2. FORMULATION OF THE PROBLEM

In this study, there are two axisymmetric strips with the same widths and infinite length in z-axis located at y=0 and y=+l planes. The widths of the strips are 2a1 and 2a2, respectively, and η denotes the normalized impedance of the strip. The geometric representation of the problem is given in Figure 2.1.

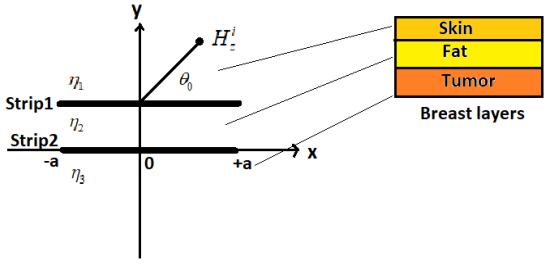

Fig. 2. Geometry of the problem.

The strip used in this study is uniform along z-axes. Therefore the problem can be formulated in 2D instead of 3D. Through the analysis, the time dependence is accepted as $exp(-i\omega t)$ for the fields, and a linearly polarized plane wave is used as the incident magnetic field as given in Eq. (2.1).

$$H_z^i(x,y) = e^{-ik(x\alpha_0 + y\sqrt{1-\alpha_0^2})} \tag{2}$$

The angle of incidence is

$$\alpha_0 = cos\theta_0. \tag{3}$$

The total field is

$$H_z(x,y) = H_z^i(x,y) + H_z^s(x,y) \tag{4}$$

where H_z^s is the scattered magnetic field by both strips. Leontovich boundary condition must be satisfied for the total field on each strip

$$\left\{\frac{\partial H_z(x,y)}{\partial y} \pm ik\eta H_z(x,y)\right\}\Big|_{y=0} = 0$$
$$x \in (-a_i, a_i), \qquad i = 1,2$$
$$\left\{\frac{\partial H_z(x,y)}{\partial y} \pm ik\eta H_z(x,y)\right\}\Big|_{y=+l} = 0 \tag{5}$$

Hence the total field can be obtained as [42]

$$H_z(x,y) = H_z^i(x,y) + \frac{1}{4}\int_{-a}^{a}\left\{kYI_m(x') - iI_e(x')\frac{\partial}{\partial y}\right\}. H_0^{(1)}\left(k\sqrt{(x-x')^2+y^2}\right)dx \tag{6}$$

where I_e and I_m are the equivalent electric and magnetic current densities, respectively and defined as follows,

$$\overline{I_e} = \hat{a}_y \times \left[\overline{H}\right]_-^+ \quad \left(\overline{H} = H\hat{a}_z\right) \tag{7}$$

$$\overline{I_e} = \hat{a}_y \times \left[H_z(x,+l) - H_z(x,0)\right] \Rightarrow$$

$$\left[H_z(x,+l) - H_z(x,0)\right]\hat{a}_x = f_2(x)\hat{a}_x \tag{8}$$

and

$$\overline{I_m} = \hat{a}_y \times \left[\overline{E}\right]_-^+ \tag{9}$$

$$i\omega\varepsilon_0\overline{E} = \nabla \times \overline{H} \qquad \overline{E} = \frac{1}{i\omega\varepsilon_0}\nabla \times \overline{H} \tag{10}$$

$$\overline{E} = \frac{1}{i\omega\varepsilon_0}\begin{pmatrix} \hat{a}_x & \hat{a}_y & \hat{a}_z \\ \frac{\partial}{\partial x} & \frac{\partial}{\partial y} & \frac{\partial}{\partial z} \\ 0 & 0 & H_z \end{pmatrix} \tag{11}$$

$$\overline{E} = \frac{1}{i\omega\varepsilon_0}\left\{\frac{\partial H_z}{\partial y}\hat{a}_x - \frac{\partial H_z}{\partial x}\hat{a}_y\right\} \tag{12}$$

$$\overline{I_m} = \frac{1}{i\omega\varepsilon_0}\left\{\frac{\partial H_z}{\partial y}\hat{a}_x - \frac{\partial H_z}{\partial x}\hat{a}_y\right\}\times\hat{a}_y \tag{13}$$

$$\overline{I_m} = \frac{1}{i\omega\varepsilon_0}\left\{\frac{\partial H(\mathrm{x},+0)}{\partial y} - \frac{\partial H(\mathrm{x},-0)}{\partial y}\right\}\hat{a}_z \tag{14}$$

$$kY = \omega\sqrt{\varepsilon_0\mu_0}\cdot\frac{1}{Z} = \frac{\omega\sqrt{\varepsilon_0\mu_0}}{\sqrt{\frac{\mu_0}{\varepsilon_0}}} = \omega\varepsilon_0 \tag{15}$$

$$\begin{aligned} kY\overline{I_m} &= \cancel{\omega\varepsilon_0}\left(\frac{1}{i\,\cancel{\omega\varepsilon_0}}\left\{\frac{\partial H(\mathrm{x},+0)}{\partial y} - \frac{\partial H(\mathrm{x},-0)}{\partial y}\right\}\right)\hat{a}_z \\ &= -i\left\{\frac{\partial H(\mathrm{x},+0)}{\partial y} - \frac{\partial H(\mathrm{x},-0)}{\partial y}\right\} \\ &= -if_1(\mathrm{x})\hat{a}_z \end{aligned} \tag{16}$$

So Eq. 2.5 can be rearranged as for first strip (a=a_1)

$$H_z(x,y) = H_z^i(x,y) - \frac{i}{4}\int_{-a}^{+a}\left\{f_1(x') + f_2(x')\frac{\partial}{\partial y}\right\}.$$

$$H_0^{(1)}(k\sqrt{(x-x')^2+y^2})dx' \tag{17}$$

All of the above steps are carried out in the second strip (a=a_2).

2.1. Boundary Conditions Applied to the problem

When the Leontovich boundary condition is rewritten for $y = +l$ and $y = 0$, Eq. (2.17) and (2.18) can be obtained by summing and subtracting the equations obtained from the boundary conditions.

$$\frac{\partial H_z(\mathrm{x},+l)}{\partial y} + ik\eta H_z(\mathrm{x},+l) = 0 \tag{18}$$

and

$$\frac{\partial H_z(\mathrm{x},0)}{\partial y} - ik\eta H_z(\mathrm{x},0) = 0 \tag{19}$$

The difference of Eq. (2.17) and Eq. (2.18) is

$$\begin{aligned} &\frac{\partial H_z(\mathrm{x},+l)}{\partial y} - \frac{\partial H_z(\mathrm{x},0)}{\partial y} \\ &+ ik\eta\left\{H_z(\mathrm{x},+l) + H_z(\mathrm{x},0)\right\} = 0 \end{aligned} \tag{20}$$

And the sum is

$$\begin{aligned} &\frac{\partial H_z(\mathrm{x},+l)}{\partial y} + \frac{\partial H_z(\mathrm{x},0)}{\partial y} \\ &+ ik\eta\left\{H_z(\mathrm{x},+l) - H_z(\mathrm{x},0)\right\} = 0. \end{aligned} \tag{21}$$

Using the expressions of the magnetic and electric current densities f_1 and f_2 in Eqs. (2.19) and (2.20)

$$f_1(\mathrm{x}) + \mathrm{ik}\,\eta\left\{H_z(\mathrm{x},+l) + H_z(\mathrm{x},0)\right\} = 0 \tag{22}$$

$$\begin{aligned} &f_2(\mathrm{x}) + \\ &\frac{1}{\mathrm{ik}\,\eta}\left\{\frac{\partial H_z(\mathrm{x},+l)}{\partial y} + \frac{\partial H_z(\mathrm{x},0)}{\partial y}\right\} = 0 \end{aligned} \tag{23}$$

are obtained.

Eqs. (2.3) and (2.16) can be used to express the total field at $y = +l$ and $y = 0$ as

$$H_z(x,+l) = H_z^i(x,+l) - \lim_{y\to+l}\frac{i}{4}\int_{-a}^{+a}\left\{ f_1(x') + f_2(x')\frac{\partial}{\partial y}\right\}. H_0^1(k|x-x'|)dx' \quad (24)$$

and

$$H_z(x,0) = H_z^i(x,0) - \lim_{y\to0}\frac{i}{4}\int_{-a}^{+a}\left\{ f_1(x') + f_2(x')\frac{\partial}{\partial y}\right\}. H_0^1(k|x-x'|)dx'. \quad (25)$$

In Eq.(2.20), we require the sum of these two expressions as

$$H_z(x,+l) + H_z(x,0) = H_z^i(x,+l) + H_z^i(x,0) - \lim_{y\to+l}\frac{i}{4}\int_{-a}^{+a}\left\{ f_1(x') + f_2(x')\frac{\partial}{\partial y}\right\}.H_0^1(k|x-x'|)dx' - \lim_{y\to0}\frac{i}{4}\int_{-a}^{+a}\left\{ f_1(x') + f_2(x')\frac{\partial}{\partial y}\right\}.H_0^1(k|x-x'|)dx' . \quad (26)$$

For the incident field we have that

$$H_z^i(\mathrm{x},l) = H_z^i(\mathrm{x},+l) = H_z^i(\mathrm{x},0) = e^{-ik\mathrm{x}\alpha_0} \quad (27)$$

and from Senior [27] we have that

$$(\lim_{y\to+l} + \lim_{y\to0})\int_{-a}^{+a}\left\{ f_2(x')\frac{\partial}{\partial y}\right\}H_0^{(1)}(\mathrm{k}|x-x'|)\,\mathrm{dx}' = 0 \quad (28)$$

and

$$\lim_{y\to+l}\int_{-a}^{+a} f_1(x')H_0^{(1)}(\mathrm{k}|x-x'|)\,\mathrm{dx}' = \lim_{y\to0}\int_{-a}^{+a} f_1(x')H_0^{(1)}(\mathrm{k}|x-x'|)\,\mathrm{dx}' = \int_{-a}^{+a} f_1(x')H_0^{(1)}(\mathrm{k}|x-x'|)\,\mathrm{dx}'. \quad (29)$$

So by substituting Eq. (2.26) on Eq. (2.27) and Eq.(2.28) into Eq. (2.25) one can get that;

$$-\frac{1}{ik\eta} f_1(\mathrm{x}) = 2\,\mathrm{H}_z^i(\mathrm{x},0) - \frac{i}{2}\int_{-a}^{+a} f_1(x')H_0^{(1)}(\mathrm{k}|x-x'|)\,\mathrm{dx}' \quad (30)$$

or

$$-\frac{1}{k\eta} f_1(\mathrm{x}) = 2ie^{-ik\mathrm{x}\alpha_0} + \frac{1}{2}\int_{-a}^{+a} f_1(x')H_0^{(1)}(\mathrm{k}|x-x'|)\,\mathrm{dx}' \quad (31)$$

Eq. (2.30) is the integral equation for the magnetic current $f_1(x)$. Using the integral representation of Hankel function at Eq. (2.31), the magnetic current in spectral-domain can be derived as an integral equation. This derivation is presented in this stage.

$$H_0^{(1)}(k|x-x'|) = \frac{1}{\pi}\int_{-\infty}^{+\infty}\frac{e^{ik(x-x')t}}{\sqrt{1-t^2}}dt. \quad (32)$$

Using Eq. (2.31) in Eq. (2.30)

$$-\frac{1}{k\eta} f_1(x) = 2ie^{-ik\mathrm{x}\alpha_0} + \frac{1}{2\pi}\int_{-a}^{+a} f_1(x')\int_{-\infty}^{+\infty}\frac{e^{ik(x-x')t}}{\sqrt{1-t^2}}dtdx' \quad (33)$$

and changing the order of integration

$$-\frac{1}{k\eta} f_1(x) = 2ie^{-ikx\alpha_0} + \frac{1}{2\pi}\int_{-\infty}^{+\infty}\left\{\int_{-a}^{+a} f_1(x')e^{-ikx't}dx'\right\}\frac{e^{ikxt}}{\sqrt{1-t^2}}dt \quad (34)$$

is obtained. Where

$$F_1(t) = \int_{-a}^{+a} f_1(x')e^{-ikx't}dx' \quad (35)$$

is the Fourier transform of the magnetic current density $f_1(x)$. So

$$-\frac{1}{k\eta} f_1(x) = 2ie^{-ikx\alpha_0} + \frac{1}{2\pi}\int_{-\infty}^{+\infty} F_m(t)\frac{e^{ikxt}}{\sqrt{1-t^2}}dt \quad (36)$$

Is derived. For the current density function to be expressed in terms of Gegenbauer polynomials, these variable changes are needed.

Since $-a \le x \le a$,

$$x = a\zeta, \quad x' = a\zeta', \quad \xi = ka$$

$$F_1(t) = \int_{-1}^{+1} f_1(a\zeta')e^{-i(\xi/a)t(a\zeta')}(ad\zeta')$$

$$F_1(t) = \int_{-1}^{+1} af_1(a\zeta')e^{-i\xi t\zeta'}d\zeta' \quad (37)$$

and let

$$\tilde{f}_1(\zeta') = af_1(a\zeta'). \quad (38)$$

So,

$$F_1(t) = \int_{-1}^{+1} \tilde{f}_1(\zeta')e^{-i\xi t\zeta'}d\zeta' \quad (39)$$

Is obtained. This means that Eq. (2.35) can be arranged as;

$$-\frac{1}{\left(\frac{\xi}{a}\right)\eta} f_1(x) = 2ie^{-i\left(\frac{\xi}{a}\right)\alpha_0(a\zeta)} + \frac{1}{2\pi}\int_{-\infty}^{+\infty} F_m(t)\frac{e^{i\left(\frac{\xi}{a}\right)(a\zeta)t}}{\sqrt{1-t^2}}dt \quad (40)$$

or

$$-\frac{1}{\xi\eta} af_1(x) = 2ie^{-i\xi\alpha_0\zeta} + \frac{1}{2\pi}\int_{-\infty}^{+\infty} F_m(t)\frac{e^{i\xi t\zeta}}{\sqrt{1-t^2}}dt \quad (41)$$

and

$$-\frac{1}{\xi\eta}\tilde{f}_1(\zeta) = 2ie^{-i\xi\alpha_0\zeta} + \frac{1}{2\pi}\int_{-\infty}^{+\infty} F_m(t)\frac{e^{i\xi t\zeta}}{\sqrt{1-t^2}}dt. \quad (42)$$

If we multiply both sides of the equation by $e^{-i\xi\beta\zeta}$ and integrate between -1 and +1

$$-\frac{1}{\xi\eta}\int_{-1}^{1}\tilde{f}_1(\zeta)e^{-i\xi\beta\zeta}d\zeta = 2i\int_{-1}^{1}e^{-i\xi\alpha_0\zeta}e^{-i\xi\beta\zeta}d\zeta + \frac{1}{2\pi}\int_{-1}^{1}e^{-i\xi\beta\zeta}\int_{-\infty}^{+\infty}F_m(t)e^{i\xi t\zeta}\frac{dt}{\sqrt{1-t^2}}d\zeta \quad (43)$$

is derived. From Eq. (2.33) it is obvious that the form on the left-hand side can be expressed as

$$F_m(\beta) = \int_{-1}^{+1}\tilde{f}_1(\zeta)e^{-i\xi\beta\zeta}d\zeta. \quad (44)$$

The first term on the right-hand side is

$$\int_{-1}^{+1}e^{-i\xi\alpha_0\zeta}e^{-i\xi\beta\zeta}d\zeta = 2\frac{\sin\xi(\beta+\alpha_0)}{\xi(\beta+\alpha_0)} \quad (45)$$

and the second term on the right-hand side by changing the order of integration;

$$\int_{-\infty}^{+\infty}\frac{F_m(t)}{\sqrt{1-t^2}}\int_{-1}^{1}e^{i\xi(t-\beta)\zeta}d\zeta\,dt=$$
$$\int_{-\infty}^{+\infty}\frac{F_m(t)}{\sqrt{1-t^2}}\left(\frac{e^{i\xi(t-\beta)\zeta}}{i(t-\beta)\xi}\right)\Bigg|_{-1}^{1}dt$$
$$=\frac{2}{\xi}\int_{-\infty}^{+\infty}\frac{F_m(t)}{\sqrt{1-t^2}}\frac{\sin\xi(t-\beta)}{(t-\beta)}dt \tag{46}$$

Is obtained. So Eq. (2.41) can be rearranged as follows to get the integral equations of the magnetic (Eq. (2.46)) and electric (Eq.(2.47)) current densities in spectral-domain

$$-\frac{1}{\xi\eta}F_m(\beta)=4i\frac{\sin\xi(\beta+\alpha_0)}{\xi(\beta+\alpha_0)}$$
$$+\frac{1}{\xi\pi}\int_{-\infty}^{+\infty}\frac{F_m(t)}{\sqrt{1-t^2}}\frac{\sin\xi(t-\beta)}{t-\beta}dt. \tag{47}$$

$$F_e(\beta)=\frac{4}{\eta}\sqrt{1-\alpha_0^{\,2}}\frac{\sin\xi(\beta+\alpha_0)}{\xi(\beta+\alpha_0)}$$
$$-\frac{1}{\pi\eta}\int_{-\infty}^{\infty}F_e(\mathrm{t})\sqrt{1-t^2}\frac{\sin\xi(\mathrm{t}-\beta)}{\mathrm{t}-\beta}dt \tag{48}$$

3. FILED ANALYSIS

The previously obtained electric F_e (β) and magnetic F_m (β) current densities can be solved by reducing these integrals to uncoupled linear algebraic equation system. Finally, these uncoupled equations can be written in the form of an infinite system of linear algebraic equations involving Gegenbauer polynomial coefficients as unknowns. The details of the intermediate steps are presented at a previous study of the author [28]. The total field expression Eq. (2.16) involving the electric and magnetic current densities as unknowns is the fundamental formula for field analysis.

$$H_z^s(\mathrm{r},\varphi)=-\frac{i}{4}\sqrt{\frac{2}{i\pi kr}}e^{ikr}$$
$$\cdot\int_{-1}^{+1}\left\{\tilde{f}_1(\zeta')+\frac{\xi\sin\varphi}{4}\tilde{f}_2(\zeta')\right\}e^{-i\xi\zeta'\cos\varphi}d\zeta'. \tag{49}$$

Then, let the scattered field be expressed as for two strips

$$H_z^s(\mathrm{r},\varphi)=A(\mathrm{kr})\phi^v(\varphi) \tag{50}$$

where,

$$A(\mathrm{kr})=\sqrt{\frac{2}{\pi kr}}e^{i(kr-\frac{\pi}{4})}\ \ and\ \ \phi^v=\phi_1^v(\varphi)+\phi_2^v(\varphi) \tag{51}$$

and,

$$\phi_i(\varphi)=\phi_{ie}(\varphi)+\phi_{im}(\varphi),\ i=1,2 \tag{52}$$

The far-field radiation pattern is represented as $\phi(\varphi)$. The integrals in Eq. (3.1) are the Fourier transforms of the current density functions. Also, $\phi_e(\varphi)$ and $\phi_m(\varphi)$ can be obtained as follows:

$$\phi_e(\varphi)=\frac{\pi}{4}\sum_{n=0}^{\infty}X_nJ_n(\xi\cos\varphi) \tag{53}$$

and,

$$\phi_m(\varphi)=\frac{\xi\sin\varphi}{4}\pi\sum_{n=0}^{\infty}Y_n\frac{J_{n+1}(\xi\cos\varphi)}{\xi\cos\varphi}. \tag{54}$$

As known the total scattering cross section can be calculated as [29],

$$\frac{\sigma_s}{4a}=-\frac{1}{\xi}\mathrm{Re}\{\phi(\theta)\} \tag{55}$$

The number of multipliers for each layer is

$$\Gamma(\omega)=\frac{Z_{layer\,2}-Z_1}{Z_{layer\,2}+Z_1} \tag{56}$$

$$Z_{layer\,2}=Z_2\frac{Z_3\cos k_{2z}l+jZ_2\sin k_{2z}l}{Z_2\cos k_{2z}l+jZ_3\sin k_{2z}l}$$
$$\eta_i:instrinsic\,impedance\,of\ ith\,layer\ (i=1,2,3)$$
$$k_{2z}:k_2\cos\theta_2\ and\ k_2:\sqrt{(\omega^2\mu_2\varepsilon_2-j\omega\mu_2\sigma_2)} \tag{57}$$

The reflected signal is shown by

$$R_0(t) = \frac{1}{2\pi}\int R_i(\omega)\Gamma(\omega)\mathrm{e}^{-j\omega t}\,d\omega \tag{58}$$

Where θ is the incident angle. For the calculation of the RCS, the values of the X_n and Y_n are needed. From the previous sections, it is clear that the determination of X_n and Y_n can be calculated numerically with $D_{ln}^{E1}, D_{ln}^{E2}, d_{ln}^{E1}$ and d_{ln}^{E2} .

For the analysis, the scattered field can be obtained numerically from the $d_{ln}^{E_{1,2}}$ and $D_{ln}^{E_{1,2}}$ functions. These equations can not be solved numerically. Therefore the calculations are evaluated using the analytical methods presented by the author at [28].

4. RESULTS

In this study, a hybrid analytical-numerical method that eliminates the disadvantages of the analytical and numerical methods which operate well at high and low frequencies, respectively, is presented. Therefore, an accurate solution for a wide frequency range is obtained. The effect of the surface impedance on the scattered far-field is investigated by considering three different mediums $\eta_1 = 1.0,\ \eta_2 = 3.0$ and $\eta_3 = 5$. From these two RCS curves of the impedance strip, the impedance of the strip surface is not affecting the backscattered field in the shadow region. Different scenarios are tested by changing the observation angle and values. Figure 1 and Figure 2 present the bistatic RCS as a function of observation angle for ka=5.0 and 15.0, respectively while θ=60° and Figure 3 and Figure 4 for the same values while θ=90°. Figure 5 and Figure 6 illustrate the monostatic RCS as a function of incidence angle for ka=5.0 and 15.0, respectively. Also, Figure 7 and Figure 8 is the total radiation pattern for ka = 0.5 and 15, respectively. Finally, Figure 9 ve Figure 10 show the bistatic RCS as a function of different ka values for θ=30° and θ=90°.

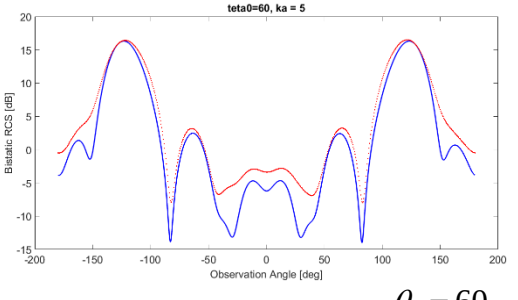

Fig. 3. Bistatic RCS [dB], ka=5.0, $\theta_0 = 60$ $(\eta_1 = 1.0\,and\,\eta_2 = 3.0; \eta_3 = 5.0)$

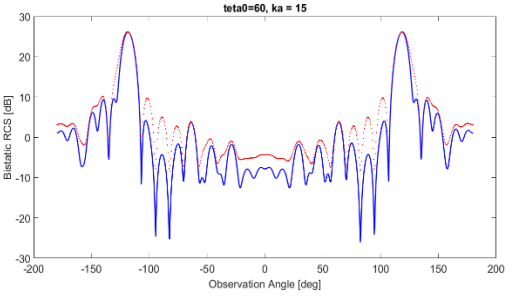

Fig. 4. Bistatic RCS [dB], ka=15.0, $\theta_0 = 60$ $(\eta_1 = 1.0\,and\,\eta_2 = 3.0; \eta_3 = 5.0)$

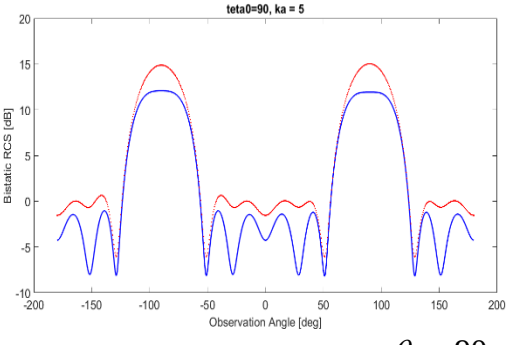

Fig. 5. Bistatic RCS [dB], ka=5.0, $\theta_0 = 90$ $(\eta_1 = 1.0\,and\,\eta_2 = 3.0; \eta_3 = 5.0)$

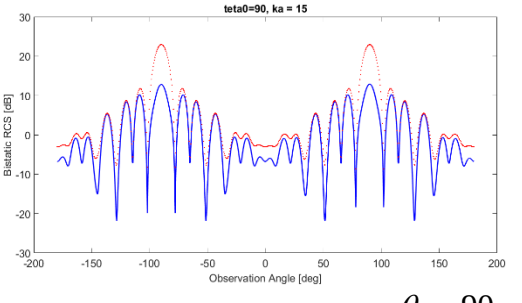

Fig. 6. Bistatic RCS [dB], ka=15.0, $\theta_0 = 90$ $(\eta_1 = 1.0\,and\,\eta_2 = 3.0; \eta_3 = 5.0)$

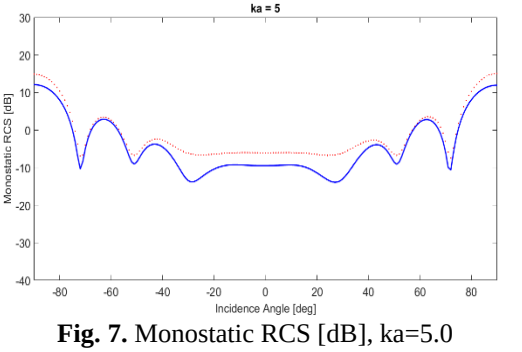

Fig. 7. Monostatic RCS [dB], ka=5.0 $(\eta_1 = 1.0\,and\,\eta_2 = 3.0; \eta_3 = 5.0)$

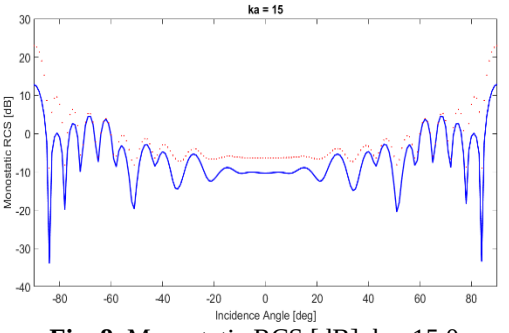

Fig. 8. Monostatic RCS [dB], ka=15.0
$(\eta_1 = 1.0 \, and \, \eta_2 = 3.0; \eta_3 = 5.0)$

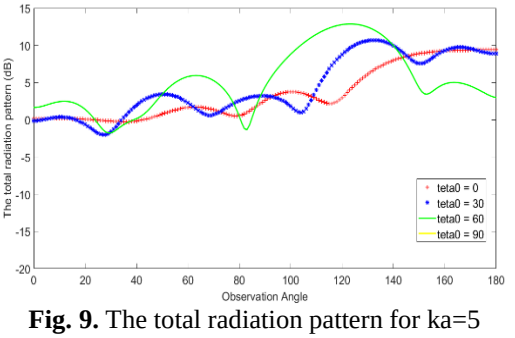

Fig. 9. The total radiation pattern for ka=5
$(\eta_1 = 1.0 \, and \, \eta_2 = 3.0; \eta_3 = 5.0)$

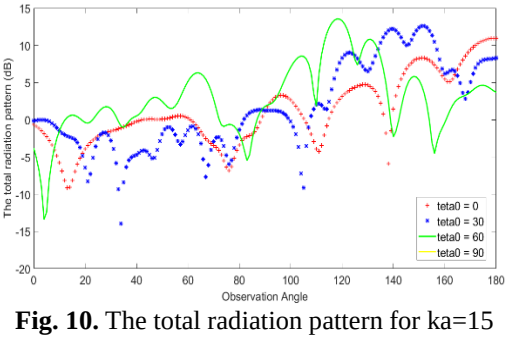

Fig. 10. The total radiation pattern for ka=15
$(\eta_1 = 1.0 \, and \, \eta_2 = 3.0; \eta_3 = 5.0)$

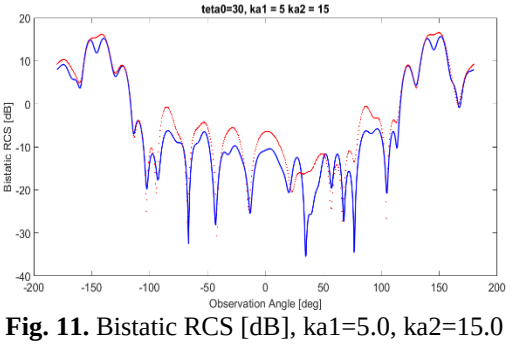

Fig. 11. Bistatic RCS [dB], ka1=5.0, ka2=15.0
$\theta_0 = 30 \;\; (\eta_1 = 1.0 \, and \, \eta_2 = 3.0; \eta_3 = 5.0)$

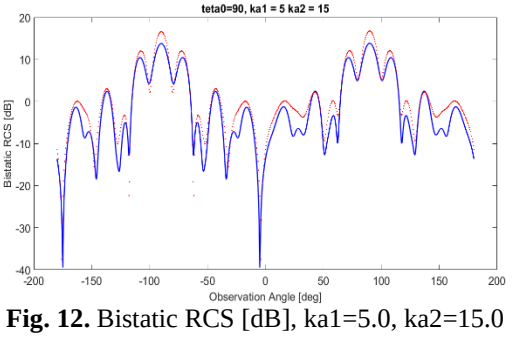

Fig. 12. Bistatic RCS [dB], ka1=5.0, ka2=15.0
$\theta_0 = 90 \;\; (\eta_1 = 1.0 \, and \, \eta_2 = 3.0; \eta_3 = 5.0)$

5. CONCLUSION

In this paper, a general model of the plane wave diffraction for detecting objects in a medium non-invasively and its solution is presented. The obtained solution is applied to detect a tumor in a breast at different observation angles and values. The diffraction problem of the H-polarized plane wave by two axisymmetric strips with varying values of impedance is considered. The magnetic and current density functions are used to formulate the problem as an integral equation. Then the boundary conditions are applied to the scattered filed, and simultaneous integral equations are obtained. The obtained integral equations which satisfied by the magnetic and electric current densities are reduced to two uncoupled infinite linear algebraic equations systems. Numerical examples with radar cross-section and total scattering field radiation patterns are presented for different scenarios. And it concluded that the proposed model could be used to detect the tumor inside a breast using microwaves.

6. ACKNOWLEDGEMENT

There is no conflict of interest.

REFERENCES

[1] E. Avşar Aydın, T. İkiz, "**An approximate solution for the plane wave diffraction by an impedance strip: H-polarization**," *Tehnicki Glasnik (Technical Journal)*, Vol. 10, pp. 79-97, 2016.

[2] Breast. (2020, October 30). Retrieved from https://en.wikipedia.org/wiki/Breast

[3] M. Born, and E. Wolf, "**Principles of Optics,"** *Pergamon Press*, Frankfurt, Germany, pp.808, 1965

[4] J. J. Bowman, "**High-frequency backscattering from an absorbing infinite strip with arbitrary face impedance**," *Canadian Journal of Phys*., Vol. 45, pp. 2409-2430, 1967.

[5] C. M. Butler,"**General solution of the narrow strip integral equations,"** *IEEE Trans. On Ant. And Proc*. Vol. AP-33, pp. 10:1085-1090, 1985

[6] A. Büyükaksoy, A. H. Serbest, A. H. and G. Uzgören, "**Secondary diffraction of plane waves by an impedance strip**,"*Radio Science*, Vol. 24, pp. 455-464,

1989.

[7] W. D. Burnside, C. L. Yu, R. J. Marhefka, "**A technique to combine the geometrical theory of diffraction and the moment method***," IEEE Trans. on Ant. and Proc*., Vol. AP-23, pp. 551-558, 1975

[8] F. Delbary, M. Brignone, G. Bozza, R. Aramini, M. Piana, "**A Visualization Method for Breast Cancer Detection by using Microwaves**," *SIAM J. Appl. Math*. Vol. 70, pp. 2509-2533, 2010.

[9] G: A. Grinberg, "**Diffraction of electromagnetic waves by strip of finite width**," *Soviet Phys. Dokland*. Vol. 4, pp. 1222-1225, 1960.

[10] A. M. Hassan, M., El-Shenawee, "**Review of Electromagnetic Techniques for Breast Cancer Detection**," *IEEE Reviews in Biomedical Engineering*, Vol. 4, pp. 103-118, 2011.

[11] M. I. Herman, J. L. Volakis, "**High frequency scattering by a resistive strip and extensions to conductive and impedance strips**, "*Radio Science*. Vol. 22, pp. 335-349, 1987.

[12] T. İkiz, S. Koshikawa, K. Kobayashi, E. İ. VelievA. H. Serbest, "**Solution of the plane wave diffraction problem by an impedance strip using a numerical-analytical method: E-polarized case**," *Journal of Electromagnetic Waves and Applications*, Vol. 15, pp. 291-436, 2001.

[13] G. A. Grinberg, "**Diffraction of electromagnetic waves by strip of finite width**," *Soviet Phys. Dokland*. Vol. 4, pp. 1222-1225, 1960.

[14] Kanser Kayıtçılığı, Türkiye Halk Sağlığı Kurumu Kanser Daire Başkanlığı (2020, October 30). Retrieved from http://www.kanser.gov.tr/dairefaaliyetleri/kanser-kayitciligi/108-t%C3%BCrkiyede.

[15] M. Kaur, M., "**Calcification Detection in Breast Cancer**," *Int. J. Psychosoc. Rehabil.* doi: 10.37200/ijpr/v24i4/pr2020377, pp. 5723–5732, 2020.

[16] A. Lazaro, D. Girbau, R. Villarino, R., "**Simulated and Experimental Wavelet-based Detection of Breast Tumor using a UWB Radar**," *40th European Microwave Conference*, Paris, pp. 373-376, 2010.

[17] L. N. Medgyesi, and D. S. Wang, "**Hybrid methods for analysis of complex scatterers,"** *Proc. of the IEEE*, vVol. 77, pp. 770-779, 1989.

[18] J. N. Sahalos, and G. A. Thiele, "**On the application of the GTD-MM technique and its limitations**," *IEEE Trans. on Ant. and Proc*., Vol. AP-29, pp. 780-786, 1981

[19] A. Santorelli, M. Popovic, M.,"**SAR Distribution in Microwave Breast Screening: Results with TWTLTLA Wideband Antenna**," *Intelligent Sensors. Sensor Networks and Information Processing (ISSNIP).* Adelaide, pp. 11-16, 2011.

[20] T. B. A. Senior, "**Backscattering from resistive strips***," IEEE Trans. on Ant. and Proc*, Vol. AP-27, pp. 808-813, 1979.

[21] T. B. A. Senior, "**Backscattering from resistive strips***," IEEE Trans. on Ant. and Proc*, Vol. AP-27, pp. 808-813, 1979.

[22] A. H. Serbest, A. Büyükaksoy, "**Some approximate methods related to the diffraction by strips and slits**, "Hashimoto, M., İdemen, M., Tretyakov, O. A.: Analytical and numerical methods in electromagnetic wave theory. *Science House*, pp. 229-256, 1987

[23] R. Tiberio, R. and R. G. Kouyoumjian," **A uniform GTD solution for the diffraction by strips illuminated at grazing incidence**," *Radio Science*, Vol. 14, pp. 933-941, 1979.

[24] G. A. Thiele, and T. H. Newhouse, "**A hybrid technique for combining moment method with the geometrical theory of diffraction**," *IEEE Trans. on Ant. and Proc*., vol. AP-23, pp. 62-69, 1975.

[25] X-ray. (2020, November 04). Retrieved from https://en.wikipedia.org/wiki/X-ray.

[26] M. Xu, P. Thulasiraman, S. Noghanian, " **Microwave Tomography for Breast Cancer Detection on Cell Broadband Engine Processors**," *J. Parallel Distrib. Comput.*, Vol. 72, ppç 1106-1116, 2011.

[27] J. L. Volakis, andS. S. Bindiganavale, "**Scattering by a narrow groove in an impedance plane**," *Radio Science*, vVol. 31, pp. 401-408, 1996.

[28] D. Zhang, A. Mase, A., "**Ultrashort-Pulse Radar System for Breast Cancer Detection Experiment: Imaging in Frequency Band**, "*Microwave Conference Proceedings (CJMW)*, Hangzhou, pp.1-3, 2011.